



Will moist convection be stronger in a warmer climate?

Anthony D. Del Genio,¹ Mao-Sung Yao,^{1,2} and Jeffrey Jonas^{1,3}

Received 27 April 2007; revised 19 June 2007; accepted 19 July 2007; published 17 August 2007.

[1] The intensity of moist convection is an important diagnostic of climate change not currently predicted by most climate models. We show that a simple estimate of the vertical velocity of convective updrafts in a global climate model reproduces observed land-ocean differences in convective intensity. Changes in convective intensity in a doubled CO₂ simulation are small because the tropical lapse rate tends to follow a moist adiabatic profile. However, updrafts strengthen by $\sim 1 \text{ m s}^{-1}$ with warming in the lightning-producing regions of continental convective storms, primarily due to an upward shift in the freezing level. For the western United States, drying in the warmer climate reduces the frequency of lightning-producing storms that initiate forest fires, but the strongest storms occur 26% more often. For the central-eastern United States, stronger updrafts combined with weaker wind shear suggest little change in severe storm occurrence with warming, but the most severe storms occur more often. **Citation:** Del Genio, A. D., M.-S. Yao, and J. Jonas (2007), Will moist convection be stronger in a warmer climate?, *Geophys. Res. Lett.*, *34*, L16703, doi:10.1029/2007GL030525.

1. Introduction

[2] It is often assumed that moist convection will be stronger in a warmer climate [e.g., *Hartmann*, 2002]. The most direct, but difficult to observe, indicator of the intensity of convection is the vertical velocity of buoyant updrafts. Updraft speed affects the detrainment of hydrometeors into anvil clouds and thus cloud feedback [*Del Genio et al.*, 2005]. It also regulates mixed-phase processes that cause lightning [*Petersen and Rutledge*, 2001]. Lightning is a leading cause of weather-related fatalities and property damage [*Curran et al.*, 2000], is a source of NO_x and O₃ [*Allen and Pickering*, 2002], and ignites forest fires [*Price and Rind*, 1994a]. Through its connection to updraft speed [*Boccippio*, 2002], lightning is sensitive to temperature and a possible indicator of climate change [*Williams*, 2005]. Only a few climate models parameterize updraft speed [*Sud and Walker*, 1999; *Donner et al.*, 2001] or treat convective microphysics. Thus models usually assume fixed precipitation efficiency and utilize indirect proxies for lightning, e.g., cloud top height [*Price and Rind*, 1994b]. Here we use a new version of the Goddard Institute for Space Studies (GISS) general circulation model (GCM) to

explain land-ocean differences in convective updraft speed and infer likely changes in a warmer climate.

2. Model and simulation description

[3] The baseline GCM is described by *Schmidt et al.* [2006] and in section S1. We run the GCM at $2^\circ \times 2.5^\circ \times 32\text{L}$ resolution. We diagnose convective updraft speed $w_c(z)$ following *Gregory* [2001]:

$$\frac{1}{2} \frac{\partial w_c^2}{\partial z} = ag \left(\frac{T'_v}{T_v} - l \right) - E(z)w_c^2 - bD(z)w_c^2 \quad (1)$$

where g is gravity, T_v is virtual temperature, the prime and overbar are in-cloud and environmental values, l is liquid water mixing ratio, $D(z)$ the fractional detrainment rate due to cloud outflow, $E(z)$ the fractional entrainment rate, and a and b are dimensionless constants. The first source term is parcel buoyancy reduced by condensate loading. The correction factor a accounts for buoyancy used for turbulence growth; without this correction the first term would convert all CAPE into updraft kinetic energy. The second term represents entrainment of environmental air into the updraft. The third term is intended to represent deceleration by cumulus-scale pressure perturbations not resolved by a GCM. Entrainment reduces parcel buoyancy by a factor C , i.e.,

$$Ew_c^2 = Cag \left(\frac{T'_v}{T_v} - l \right), \quad (2)$$

which implies that buoyancy provides the energy to accelerate entrained air to the updraft speed. We take $a = 1/6$, $b = 2/3$. (1) is integrated with w_c at cloud base determined by the boundary layer turbulent kinetic energy per unit mass (*TKE*) assuming isotropy, i.e., $w_c^2(0) = 2/3 \text{ TKE}$, for one plume and twice that speed for the other plume. We take the dimensionless constant $C = 0.6$ and 0.3 for the two plumes to give entrainment rates similar to those in tropical congestus [*Jensen and Del Genio*, 2006]. All constants have the same values over land and ocean.

[4] The parameterization has been validated against cloud resolving model and large eddy simulations [*Gregory*, 2001]. We, however, wish to apply it to thermodynamic profiles on GCM grid scales. Several studies suggest that grid scale thermal structure is relevant to the climatological diagnosis of convection [*Ye et al.*, 1998; *Brooks et al.*, 2003]. Figure 1 (see also auxiliary material¹ Table S1) shows GCM temperature errors, which in convective regions are 0.3–1.5°C at the surface (except for the United

¹NASA Goddard Institute for Space Studies, New York, New York, USA.

²Sigma Space Partners, LLC, New York, New York, USA.

³Columbia University, New York, New York, USA.

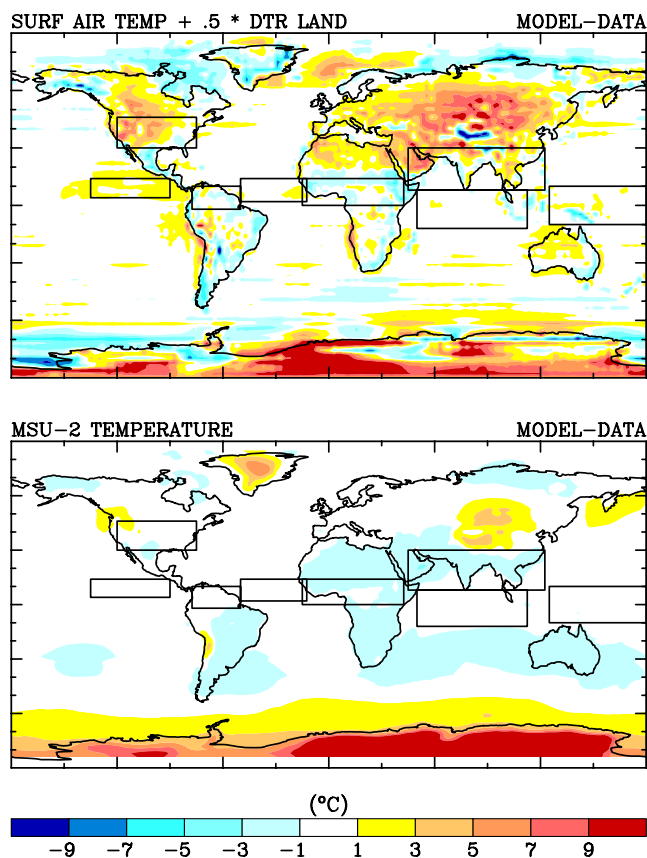


Figure 1. June–July–August differences between GCM and observed [Jones *et al.*, 1999] maximum surface air temperature (upper) and between GCM and observed [Shah and Rind, 1995] mid-troposphere temperature (lower). Maximum surface temperature is the daily mean plus half the diurnal temperature range. Boxes delineate regions in which updraft speeds are analyzed: Equatorial Africa, Amazon Basin, South Asia, United States, East Pacific Intertropical Convergence Zone (ITCZ), Atlantic ITCZ, Indian Ocean ITCZ, and West Pacific Warm Pool.

States, which is 2.8°C too warm) and $0\text{--}1.6^{\circ}\text{C}$ in the mid-troposphere. Regional lapse rate errors are $\sim 0.1\text{--}0.5^{\circ}\text{C km}^{-1}$, but land-ocean differences are close to that observed. Low-level specific humidities (not shown) are within $\sim 1\text{ g kg}^{-1}$ of ERA-40 reanalysis values.

[5] We compare a current climate run with climatological sea surface temperature (SST) to a proxy warmer climate simulation with doubled CO_2 and SSTs the same as in a $2 \times \text{CO}_2$ run with the baseline GCM, whose climate sensitivity is 2.7°C . Results are averages over the last 5 years of a 6-year simulation.

3. Regional Variation of Updraft Speeds

[6] For June–August we define 4 regions each over land and ocean (Figure 1) encompassing the major locations of deep convection. Figure 2 shows GCM mean updraft speed profiles for deep convection in the current and warmer climate. Zipser and Lutz [1994] show composite field

experiment profiles with vertical velocities near the freezing level of $10\text{--}12\text{ m s}^{-1}$ for updraft cores over land and $4\text{--}5\text{ m s}^{-1}$ over ocean. GCM continental updraft speeds are slightly lower but clearly capture the land-ocean difference. Peak instantaneous updraft speeds over land (see Figure 3) are tens of m s^{-1} , as observed [Cotton and Anthes, 1989]. Ocean updrafts decelerate near the freezing level and re-intensify above as ice forms [Simpson and Wiggert, 1969], while more buoyant land updrafts accelerate continuously into the upper troposphere.

[7] Zipser *et al.* [2006] find the United States and Africa to have the most intense thunderstorms on Earth. Our updrafts are slightly stronger over the U.S. but only $\sim 1/2$ as frequent there as over Africa. Updrafts over the more maritime Amazon “green ocean” [Williams *et al.*, 2002] are $\sim 1\text{--}2\text{ m s}^{-1}$ weaker than over Africa. South Asian updraft speeds (auxiliary material Figure S1) are too strong, due to the overestimated lapse rate there (auxiliary material Table S1). The West Pacific profile in Figure 2 is representative of the East Pacific, Atlantic, and Indian Ocean as well (auxiliary material Figure S1).

[8] GCM updrafts are stronger over land than ocean solely because of land-ocean differences in thermodynamic profiles. The updrafts are most sensitive to the thermal structure below the freezing level, which controls the acceleration due to buoyancy (T'_v). Convective available potential energy (CAPE), which depends in addition on cloud top height and upper level lapse rates, differs less between land and ocean [Williams and Stanfill, 2002] and is a poorer indicator. The GCM does not represent land-ocean differences in turbulent parcel size or cloud base height [Williams and Stanfill, 2002], nor does it include aerosol influences on microphysics, which may affect intensity as well [Rosenfeld and Lensky, 1998; Michalon *et al.*, 1999].

[9] Zipser and Lutz [1994] suggest a threshold updraft speed of $6\text{--}7\text{ m s}^{-1}$ for the occurrence of lightning. A 7 m s^{-1} threshold in the GCM implies that lightning occurs in 30% (Africa), 16% (Amazon), and 2% (West and East Pacific) of storms. Tropical Rainfall Measuring Mission (TRMM) data [Nesbitt *et al.*, 2000] indicate 16%, 12%, 0.3%, and 0.2% of all precipitation features with detected lightning in the same regions. The larger GCM frequencies may not be unrealistic since the updraft threshold is approximate, TRMM does not detect flash rates $< 1\text{ flash min}^{-1}$, and TRMM sees only a snapshot of each storm, including some stratiform anvils after convection and lightning have ceased. Rather than using updraft speeds directly, it might be possible instead to use their effect on the vertical profile of large hydrometeors to parameterize lightning as a function of the radar echo top [Futyan and Del Genio, 2007].

4. Climate Changes in Cumulus Updraft Strengths

[10] Figure 2 shows that for the $2 \times \text{CO}_2$ simulation, the largest increases in continental updraft speed with warming occur in the upper troposphere, due to increased CAPE. Near the freezing level increases are 0.5 m s^{-1} or less. However, the freezing level rises by $40\text{--}50\text{ mb}$ with warming. Since continental convective parcels are buoyant and thus accelerate in mid-troposphere, the higher freezing level adds another $\sim 0.5\text{ m s}^{-1}$ to the effective change in

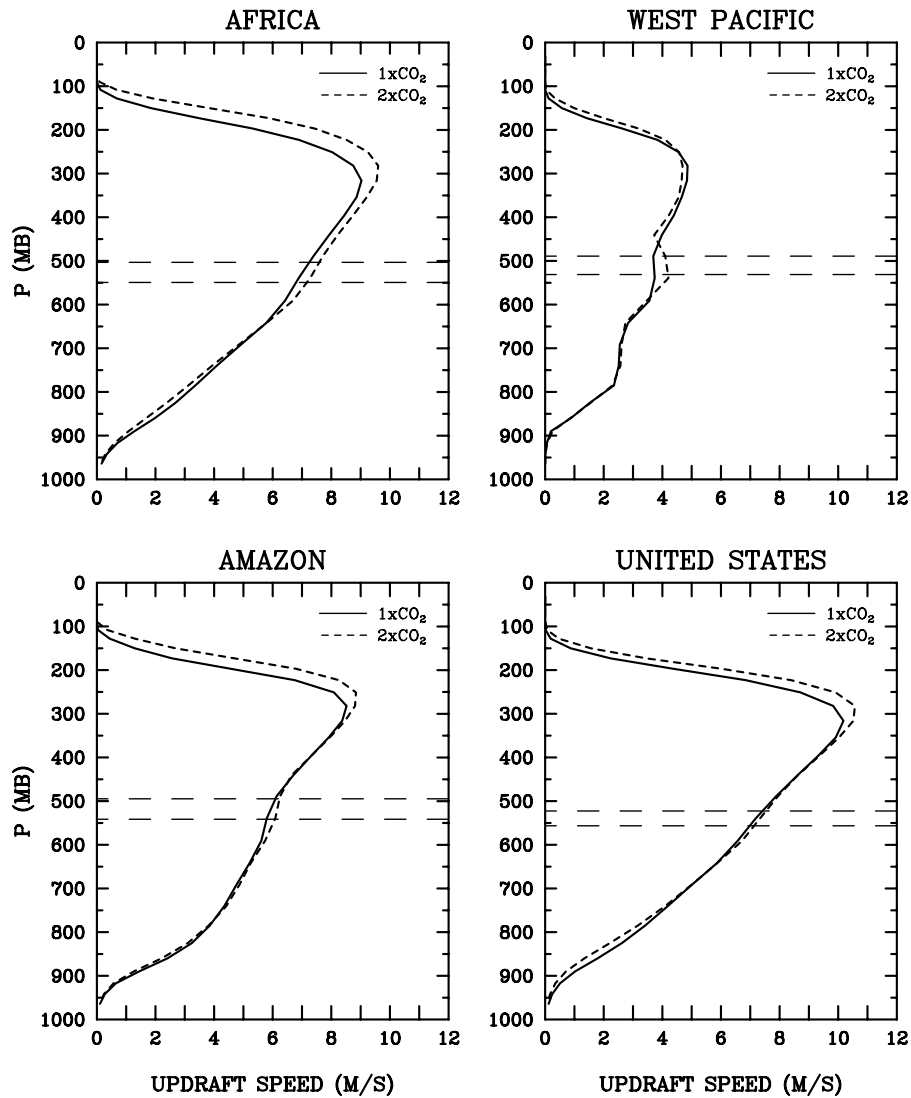


Figure 2. Current climate (solid) and $2 \times \text{CO}_2$ (dashed) mean updraft speed profiles for all deep convective events for the Africa, West Pacific, Amazon, and United States regions. Horizontal lines indicate the freezing level, the lower one in each panel for the current climate.

updraft speed. Thus, warmer climate updrafts are $\sim 1 \text{ m s}^{-1}$ stronger than control climate updrafts at their respective freezing levels. Though small, the changes are evident after averaging results over two summers or more. Ocean updrafts are nearly neutrally buoyant in mid-troposphere, so the total change in updraft speed is $\sim 0.5 \text{ m s}^{-1}$ or less. Updrafts $> 7 \text{ m s}^{-1}$ occur $\sim 10\%$ more often over land, and 0–2% more often over ocean, in the warmer climate.

[11] Climate models simulate tropical lapse rate changes that closely follow the moist adiabatic lapse rate, particularly over ocean. If lapse rate follows a moist adiabat exactly, there is no temperature contribution to buoyancy change, only small compensating effects of the cloud-environment water vapor difference and condensate loading (see section S3). In reality, tropical lapse rates deviate from moist adiabatic and thus the small temperature contribution to buoyancy determines changes in updraft speed, especially over land, where surface temperature warms 1.4°C more than over ocean, a robust feature of climate models. Sensitivity tests show these features to be robust to large

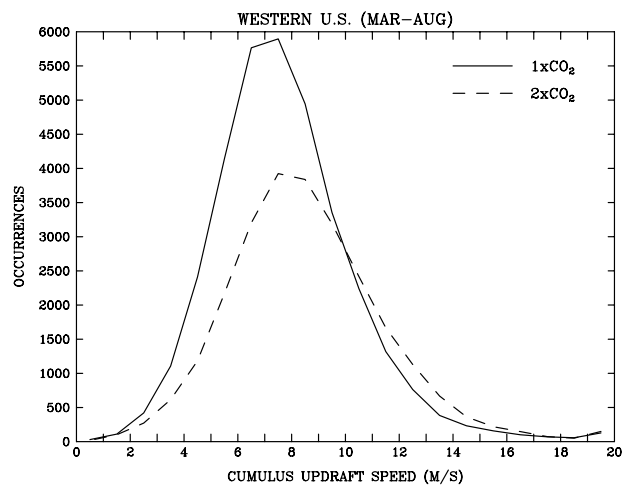


Figure 3. Histograms of GCM deep convection freezing level updraft speed occurrence for the current (solid) and warmer (dashed) climates for the western U.S. Occurrences $> 20 \text{ m s}^{-1}$ have been added to the highest updraft speed bin.

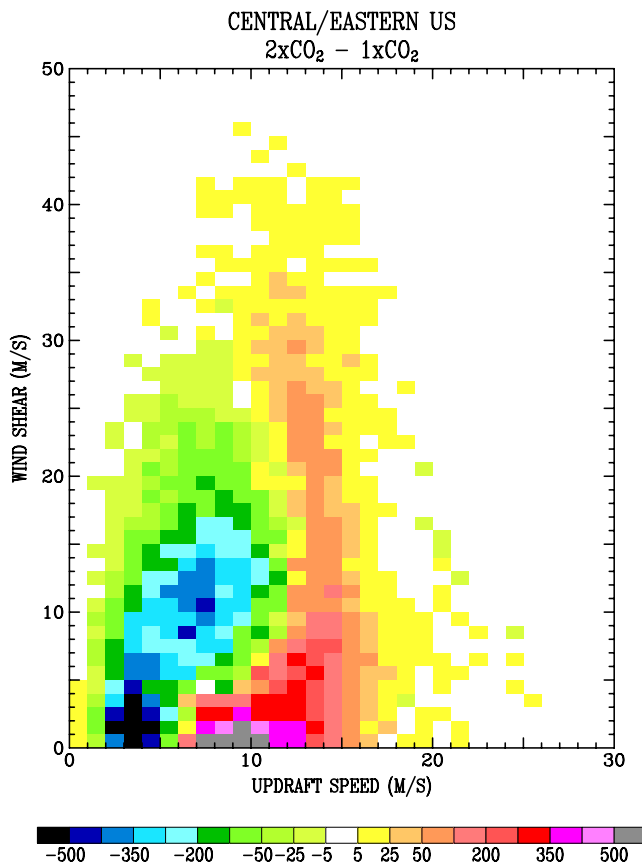


Figure 4. Occurrence difference in simultaneous values of updraft speed and 0–6 km horizontal wind speed difference magnitude for the warmer minus the current climate for the central/eastern United States for March–August.

changes in the free parameters of the parameterization (see auxiliary material Text S1, section 3).

[12] The mean updraft changes are small, but changes in the tails of the distribution can have important consequences. To illustrate we divide the U.S. into west and central/east subregions, divided by the Rocky Mountains. Forest fire activity and burned area in the western U.S. and Canada have increased in recent decades due to climate warming and drying [Gillett *et al.*, 2004; Westerling *et al.*, 2006]. Do climate changes in lightning, the primary ignition source for wildfires, play a role?

[13] Figure 3 shows frequency distributions of freezing level updraft speeds for the western region in the current and warmer climates. The GCM has a summer warm bias here (Figure 1), so the behavior may be exaggerated. In the warmer climate, surface relative humidity decreases by $\sim 2\%$ and convection with updraft speeds $> 7 \text{ m s}^{-1}$ occurs 9% less often. However, strong events ($> 10 \text{ m s}^{-1}$, the upper 16%) occur 26% more often. Boccippio’s [2002] “most consistent” estimate for flash rate $F = 1.52 \times 10^{-3} w_c^{2.67}$ applied to Figure 3 predicts a 6% increase in western U.S. lightning for the warmer climate. Thus, changes in lightning ignition of western wildfires may enhance the climate change in burned area caused by drying.

[14] The central/east U.S. experiences the most severe thunderstorms and tornadoes on Earth [Doswell, 2001] due to its unique combination of steep lapse rates, moist boundary layer inflow, and substantial wind shear. Brooks *et al.* [2003] show that severe weather “favorable day” indices from global reanalyses predict the climatological locations and seasonal cycle of observed severe weather. Their simplest index indicates that CAPE and 0–6 km wind shear together provide a good discriminator for severe weather.

[15] Updraft speed is a more direct indicator of convective intensity than CAPE. Figure 4 shows the climate change in the occurrence of simultaneous updraft speed and shear values for March–August, the primary severe weather season. Increased updraft strength combined with weaker wind shear due to polar amplification of warming imply that on balance severe weather will change little as climate changes, with less/more contribution from shear vorticity and instability, respectively. However, Figure 4 also shows a systematic increase in the highest shear ($> 30 \text{ m s}^{-1}$), strongest updraft ($> 7 \text{ m s}^{-1}$) occurrences of severe conditions. This occurs because latent heating increasingly contributes to the generation of available potential energy. Temperature gradients and wind shears may increase with warming only in lifted frontal air, precisely where thunderstorms should strengthen. Thus, winds and severe weather may intensify locally in the midst of a general decrease in synoptic wind shear as climate warms.

5. Conclusions

[16] A simple diagnosis of cumulus updraft speed that depends only on the large-scale thermodynamic structure reproduces the observed magnitude and land-ocean differences in convective intensity in a GCM. The model predicts more intense convection (by $\sim 1 \text{ m s}^{-1}$) in a warmer climate over land. Decreases in convection frequency with warming partly offset the effect of stronger convection, but the nonlinear dependence of lightning on updraft speed implies higher flash rates overall. Midlatitude severe weather may also not change dramatically, but the most severe storms may occur more often.

[17] Our ability to explain land-ocean differences in convective intensity as a result of thermal structure differences does not imply that other factors such as cloud base height and aerosol concentration do not play a role. Nonetheless, updraft speed shows promise as a more physical way to diagnose lightning sources of forest fires and related aerosol and greenhouse gas sources in GCMs than simply using convective cloud top height as a proxy.

[18] **Acknowledgments.** This work was supported by the NASA Modeling and Analysis and Precipitation Science Programs and the DOE Atmospheric Radiation Measurement Program. Ann Fridlind, Earle Williams and another reviewer provided helpful comments.

References

- Allen, D. J., and K. E. Pickering (2002), Evaluation of lightning flash rate parameterizations for use in a global chemical transport model, *J. Geophys. Res.*, 107(D23), 4711, doi:10.1029/2002JD002066.
- Boccippio, D. J. (2002), Lightning scaling relations revisited, *J. Atmos. Sci.*, 59, 1086–1104.

- Brooks, H. E., J. W. Lee, and J. P. Craven (2003), The spatial distribution of severe thunderstorm and tornado environments from global reanalysis data, *Atmos. Res.*, *67–68*, 73–94.
- Cotton, W. R., and R. A. Anthes (1989), *Storm and Cloud Dynamics*, Academic Press, San Diego, Calif.
- Curran, E. B., R. L. Holle, and R. E. López (2000), Lightning casualties and damages in the United States from 1959 to 1994, *J. Clim.*, *13*, 3448–3464.
- Del Genio, A. D., W. Kovari, M.-S. Yao, and J. Jonas (2005), Cumulus microphysics and climate sensitivity, *J. Clim.*, *18*, 2376–2387.
- Donner, L. J., C. J. Seman, and R. S. Hemler (2001), A cumulus parameterization including mass fluxes, convective vertical velocities and mesoscale effects: Thermodynamic and hydrological aspects in a general circulation model, *J. Clim.*, *14*, 3444–3463.
- Doswell, C. A., III (2001), *Severe Convective Storms*, *Meteorol. Monogr. Ser.*, vol. 28(50), 570 pp., Am. Meteorol. Soc., Boston, Mass.
- Futyan, J. M., and A. D. Del Genio (2007), Parameterizing lightning in current and future GCMs, *Geophys. Res. Lett.*, *34*, L15705, doi:10.1029/2007GL030227.
- Gillett, N. P., A. J. Weaver, F. W. Zwiers, and M. D. Flannigan (2004), Detecting the effect of climate change on Canadian forest fires, *Geophys. Res. Lett.*, *31*, L18211, doi:10.1029/2004GL020876.
- Gregory, D. (2001), Estimation of entrainment rate in simple models of convective clouds, *Q. J. R. Meteorol. Soc.*, *127*, 53–72.
- Hartmann, D. L. (2002), Tropical surprises, *Science*, *295*, 811–812.
- Jensen, M. P., and A. D. Del Genio (2006), Factors limiting convective cloud-top height at the ARM Nauru Island climate research facility, *J. Clim.*, *19*, 2105–2117.
- Jones, P. D., M. New, D. E. Parker, S. Martin, and I. Rigor (1999), Surface air temperature and its variations over the last 150 years, *Rev. Geophys.*, *37*, 173–199.
- Michalon, N., A. Nassif, T. Saouri, J. F. Royer, and C. A. Pontikis (1999), Contribution to the climatological study of lightning, *Geophys. Res. Lett.*, *26*, 3097–3100.
- Nesbitt, S. W., E. J. Zipser, and D. J. Cecil (2000), A census of precipitation features in the tropics using TRMM: Radar, ice scattering, and lightning observations, *J. Clim.*, *13*, 4087–4106.
- Petersen, W. A., and S. A. Rutledge (2001), Regional variability in tropical convection: Observations from TRMM, *J. Clim.*, *14*, 3566–3586.
- Price, C., and D. Rind (1994a), The impact of a $2 \times \text{CO}_2$ climate on lightning-caused fires, *J. Clim.*, *7*, 1484–1494.
- Price, C., and D. Rind (1994b), Possible implications of global climate change on global lightning distributions and frequencies, *J. Geophys. Res.*, *99*, 10,823–10,831.
- Rosenfeld, D., and I. M. Lensky (1998), Satellite-based insights into precipitation formation processes in continental and maritime convective clouds, *Bull. Am. Meteorol. Soc.*, *79*, 2457–2476.
- Schmidt, G. A., et al. (2006), Present-day atmospheric simulations using GISS Model E: Comparison to in situ, satellite, and reanalysis data, *J. Clim.*, *19*, 153–192.
- Shah, K. P., and D. Rind (1995), Use of microwave brightness temperatures with a general circulation model, *J. Geophys. Res.*, *100*, 13,841–13,874.
- Simpson, J., and V. Wiggert (1969), Models of precipitating cumulus towers, *Mon. Weather Rev.*, *97*, 471–489.
- Sud, Y. C., and G. K. Walker (1999), Microphysics of clouds with the relaxed Arakawa-Schubert scheme (McRAS). Part I: Design and evaluation with GATE Phase III data, *J. Atmos. Sci.*, *56*, 3196–3220.
- Westering, A. L., H. G. Hidalgo, D. R. Cayan, and T. W. Sweetnam (2006), Warming and earlier spring increase western U.S. forest wildfire activity, *Science*, *313*, 940–943.
- Williams, E. (2005), Lightning and climate: A review, *Atmos. Res.*, *76*, 272–287.
- Williams, E., and S. Stanfill (2002), The physical origin of the land-ocean contrast in lightning activity, *C. R. Phys.*, *3*, 1277–1292.
- Williams, E., et al. (2002), Contrasting convective regimes over the Amazon: Implications for cloud electrification, *J. Geophys. Res.*, *107*(D20), 8082, doi:10.1029/2001JD000380.
- Ye, B., A. D. Del Genio, and K. K.-W. Lo (1998), CAPE variations in the current climate and in a climate change, *J. Clim.*, *11*, 1997–2015.
- Zipser, E. J., and K. R. Lutz (1994), The vertical profile of radar reflectivity of convective cells: A strong indicator of storm intensity and lightning probability?, *Mon. Weather Rev.*, *122*, 1751–1759.
- Zipser, E. J., D. J. Cecil, C. Liu, S. W. Nesbitt, and D. P. Korty (2006), Where are the most intense thunderstorms on Earth?, *Bull. Am. Meteorol. Soc.*, *87*, 1057–1071.

A. D. Del Genio, J. Jonas, and M.-S. Yao, NASA Goddard Institute for Space Studies, 2880 Broadway, New York, NY 10025, USA. (adelgenio@giss.nasa.gov)